Journal of Power Sources, 18 (1986) 317 - 335

DEVELOPMENT OF LOW COST ALKALINE FUEL CELLS

K. TOMANTSCHGER*, F. McCLUSKY, L. OPORTO and A. REID

Institute for Hydrogen Systems, 2480 Dunwin Drive, Mississauga, Ontario L5L 1J9 (Canada)

K. KORDESCH

Technical University Graz, A-8010 Graz (Austria)

(Received February 4, 1986; in revised form April 29, 1986)

Summary

Fuel cells as direct energy converters will find wide application in a future hydrogen economy. At the Institute for Hydrogen Systems (IHS) emphasis was placed on designing a mass producible, low, cost, alkaline, bipolar fuel cell. Carbon-filled plastics are used in the construction of the fuel cell stack. Teflon bonded, multilayer carbon electrodes have been developed. The pretreatment of carbon materials proved necessary to prolong the life of the electrodes. Electrocatalysis work resulted in the replacement of the noble metal electrocatalyst of the cathode and a significant reduction in the loading of the anode. The material cost of the alkaline, bipolar hydrogen–air fuel cell currently stands at Can $250 (US $175) per kW.

Introduction

The use of hydrogen as a universal fuel in regions with access to plentiful reserves of renewable energy seems very attractive [1]. In a hydrogen-based economy, the chemical energy stored in hydrogen fuel can be directly converted into electricity via a fuel cell. The electrochemical reaction of hydrogen and air to form water in a fuel cell is not limited by Carnot's law and the efficiency of conversion of chemical energy of the hydrogen fuel into electricity is therefore very high: under practical conditions 50 - 65% is achieved in fuel cells, compared with 15 - 25% in an internal combustion engine.

Fuel cells are generally classified by the electrolyte used and/or the operating temperature. Electricity can be produced from hydrocarbon fuels in phosphoric acid fuel cells at 200 °C (medium operating temperature) after passing through a reformer [2, 3]. Units up to several megawatt power output have been successfully operated [4, 5]. Low temperature (50 - 100 °C) solid polymer electrolyte (SPE) fuel cells operating on hydrogen supplied from a methanol cracking unit have been developed by General Electric [6, 7]. Low temperature alkaline fuel cell systems achieved fame in the

*Present address: Astris Science Inc., 2480 Dunwin Drive, Mississauga, Ontario L5L 1J9, Canada.

0378-7753/86/$3.50

1960s during the NASA Apollo program which placed man on the moon. Today, the alkaline fuel cell is still the workhorse of the space shuttle [8]. Alkaline fuel cells for terrestrial applications have been developed in Europe [9, 10]. Recent research and development efforts include molten carbonate fuel cells with the potential for clean and efficient generation of electricity from hydrocarbon and coal at 650 °C (high operating temperature) [11], and the solid oxide system, a natural gas or volatile-liquid-fueled power generator, operating with high efficiency at 1000 °C [12].

Early alkaline cells were constructed with electrodes having metallic support structures. Edge collection could be used to current densities up to 100 mA cm^{-2}. Acidic cells which could not use metals employed all-carbon construction in the bipolar design. For low cost production, the bipolar concept has been applied to alkaline fuel cells. The present design makes use of low cost thermoplastic and conductive plastic materials. A mass producible, high performance, low cost multicell has been developed. Different power sizes are achieved through a modular arrangement. Figure 1 shows the applications defined by a user group [13].

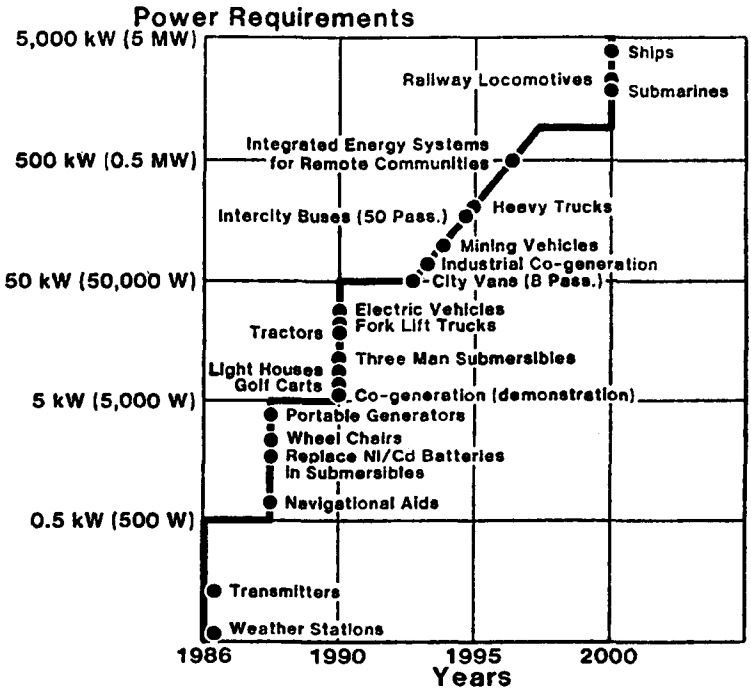

Fig. 1. Applications for alkaline bipolar fuel cells.

Construction of the multicell stack

The construction and principal operation of the alkaline hydrogen–air fuel cell is shown in Fig. 2 [14, 15]. Hydrogen and air are fed to porous

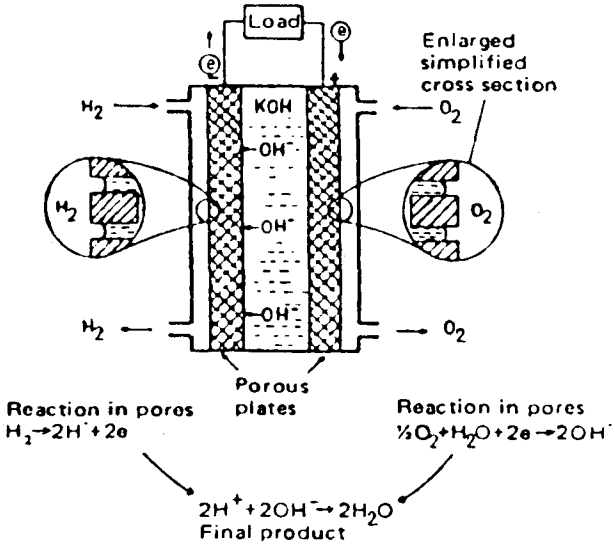

Fig. 2. Operation principle of H_2–O_2 fuel cell.

gas diffusion electrodes where oxygen reduction and hydrogen oxidation occur producing electrical power. The IHS uses the circulating electrolyte concept. Although electrolyte circulation increases design complexity, it removes reaction products, assists in thermal management, and ensures an homogeneous electrolyte. Figure 3 shows a block diagram of a conceptual design for a hydrogen–air fuel cell power plant. In the hydrogen loop, hydrogen gas enters the battery block where it is uniformly distributed to the cells. Hydrogen leaving the fuel cell stack contains water which is removed in a condenser. Hydrogen circulation is achieved by means of a jet pump. A blower motor forces air into a CO_2 scrubber, from where the air is directed into the air-intake manifolds of the fuel cell stack. Moisture-

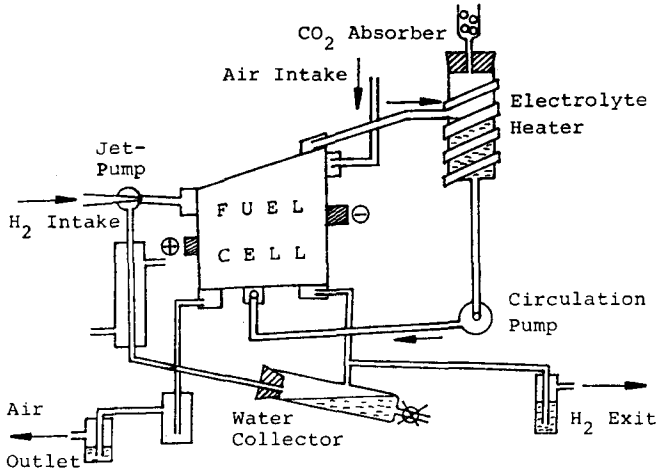

Fig. 3. Schematic of an alkaline fuel cell system.

laden air is exhausted to atmosphere. The electrolyte circulation loop consists of a reservoir, an electrolyte pump, and a heat exchanger for initial heating and cooling purposes. Figure 4 shows a multicell stack design.

The IHS design makes use of the bipolar plate construction in order to reduce internal resistance, avoid expensive metal current collectors, and allow mass production. Figure 5 shows the electrode arrangement in the alkaline bipolar cell. The bipolar plates make use of polypropylene composite materials with conductivity in the range 0.1 - 1.0 ohm cm. Recessed bipolar plates eliminate the necessity for electrolyte frames, reducing the multicell components to bipolar plates, electrodes, and endplates.

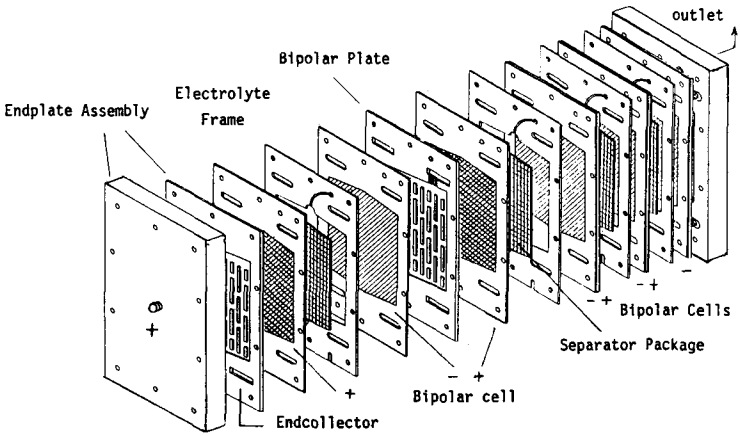

Fig. 4. Five cell alkaline fuel cell stack.

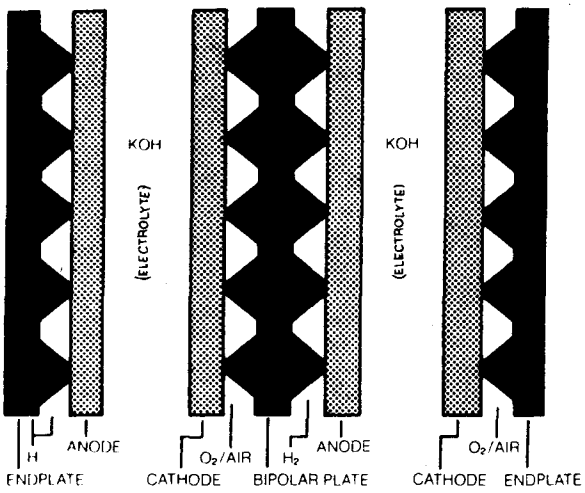

Fig. 5. Electrode arrangement of a bipolar fuel cell.

Four components contribute to the *IR* losses in each unit cell. The contribution from the *bipolar plate* is minimized by using highly conductive composite materials, careful design of plate thickness and geometry, and, if necessary, metal plating [16].

The *contact* resistance between the electrode and the bipolar plate requires special attention. The methods evaluated so far include pressure contacts and gluing techniques. Chromic acid etching and/or sandblasting techniques are used to remove the non-conductive surface film on the bipolar plate. In the case of a pressure contact, spacers are placed in the electrolyte compartment to maintain the contact pressure. Bonding the electrodes to the bipolar plate with epoxy (either conducting or non-conducting) also gives a durable contact. The *IR* losses, in a contact made with a silver-filled epoxy, are shown for a cathode endplate (Fig. 6) and an anode endplate (Fig. 7). The 5 mV contact loss at current densities of 100 mA cm^{-2} can also be achieved using non-conductive epoxy. Figure 8 shows the *IR* losses of a cathode endplate as a function of the operating current density. Presently, carbon cloth is used as electrode backing. The bipolar plate is silver plated on the air side and nickel plated on the hydrogen side. Further development is aiming to eliminate metal coatings on the bipolar plate.

The *IR* loss in the *electrodes* was found to be below 5 mV at a current density of 100 mA cm^{-2} after the electrodes are properly wetted.

The thickness of the *electrolyte* compartment and the conductivity of the KOH determine the *IR* loss in the electrolyte. The maximum conductivity of the KOH/water mixture lies at 7 N. The IHS fuel cell begins

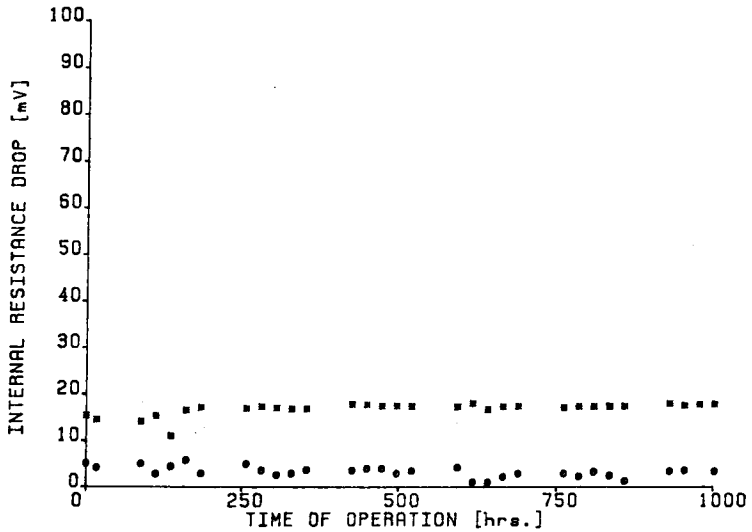

Fig. 6. Internal resistance evaluation of a cathode endplate at a current density of 100 mA cm^{-2} (12 N KOH, 65 °C). A batch 702 electrode, operating on air, is attached to a 10 cm^2 Ag-plated SX.1 conductive plastic endplate using RBC Ag-epoxy. The *IR* losses in the endplate (*) and in the contact (●) are shown as a function of the operating time.

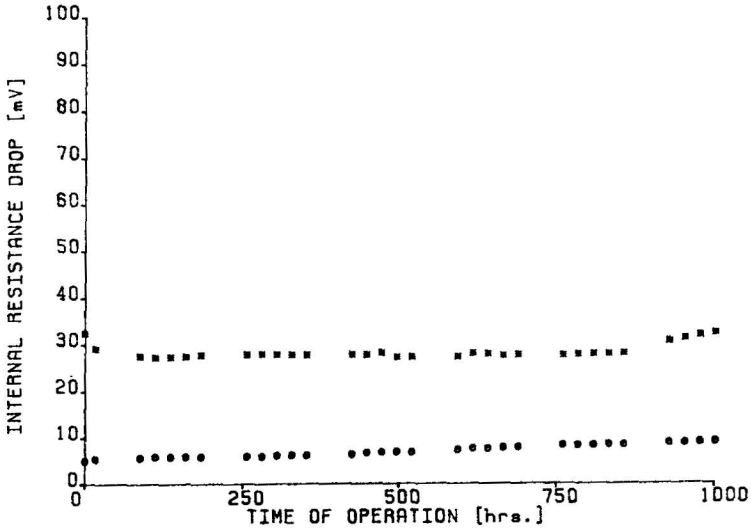

Fig. 7. Internal resistance evaluation of an anode endplate at a current density of 100 mA cm^{-2} (12 N KOH, 65 °C). A batch 23H2 electrode is attached to a 10 cm^2 Ag-plated SX.1 conductive plastic endplate using RBC Ag-epoxy. The *IR* losses in the endplate (*) and in the contact (●) are shown as a function of the operating time.

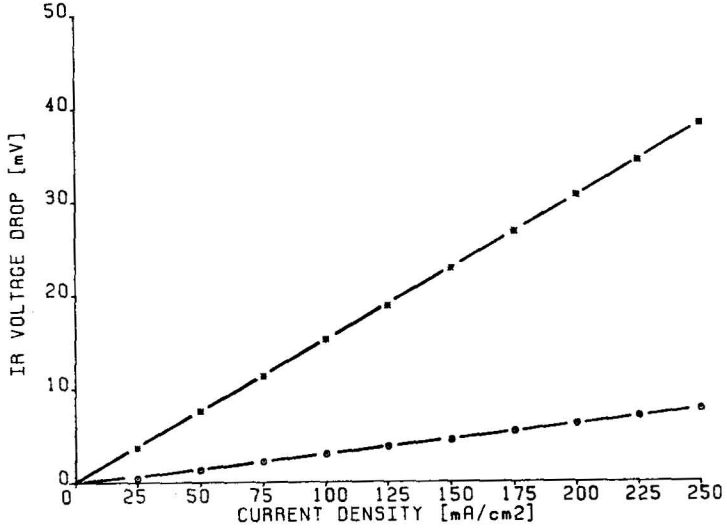

Fig. 8. Voltage drop in a bipolar plate assembly as a function of the current density using conductive epoxy contacts [16]. A batch 902 electrode, operating on air, is attached to a 10 cm^2 Ag-plated SX.1 conductive plastic endplate using RBC Ag-epoxy. The *IR* losses in the endplate (*) and in the contact (●) are shown as a function of the current density.

its operation with 12 N KOH electrolyte, but dilution occurs during operation. Depending on various operating parameters, the electrolyte concentration equilibrates in the range 7 - 9 moles of KOH per litre.

To date, the total *IR* loss in the IHS alkaline bipolar fuel cell, during operation at 100 mA cm^{-2}, lies in the range 100 - 150 mV. At 100 mA cm^{-2} ten cell multicell stacks have been successfully operated at 7 V and an *IR* loss of approx. 200 mV per cell. Present work indicates that the *IR* drop can be halved in the near future [16].

Using mass production techniques at high volume component production, the material cost for the IHS alkaline bipolar fuel cells are projected to be Can $250 per kW.

Electrode design

Teflon bonded, multilayer carbon electrodes have been developed [17 - 19]. Material selection and pretreatment is given prime importance [20 - 22]. Carbon materials used are acetylene blacks (Shawinigan SH100) and furnace blacks (Vulcan XC72R). All carbon materials are subjected to thermal treatment in steam or CO_2 atmospheres. These treatments (especially in the presence of spinels or noble metal catalysts) double the BET surface area, oxidizing "unstable carbon", and depositing new pyrolytic carbon [23].

Teflon is used to achieve hydrophobicity, and as a binder material, although polyethylenes/polypropylenes are being investigated. A cross section of the Teflon bonded multilayer carbon electrodes is shown in Fig. 9. The electrode backing should have high permeability to gases, structural strength, corrosion resistance, and high conductivity. The bipolar construction allows the use of carbon cloth or porous carbon paper, as well as metal screens. The diffusion layer consists of carbon and 30 - 50% Teflon. In order to provide the necessary pores for gas diffusion, filler materials (am-

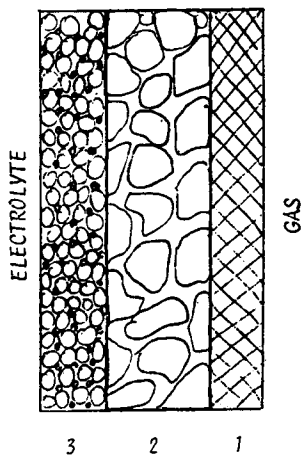

Fig. 9. Cross section of a Teflon bonded multilayer carbon electrode: 1, backing; 2, gas diffusion layer; 3, catalyst layer.

monium bicarbonate) are used in the air cathode. The electrocatalyst layer is less wetproofed than the diffusion layer (10 - 20% Teflon) to ensure partial wetting of the carbon and the electrocatalyst particles [19]. In the catalyst layer, a three phase reaction zone (where gaseous fuel, electrolyte and carbon supported electrocatalyst meet) is created.

The first generation electrodes met the set 2000 h lifetime goal at a nominal current density of 100 mA cm^{-2} in 12 N KOH at 65 °C utilizing noble metal electrocatalysts. On the air cathode 0.5 mg of Pt per cm^2 were applied and 1 mg Pd/Rh per cm^2 on the anode. Electrocatalysis work carried out has shown that especially activated carbon catalyzes the first step of the oxygen reduction to the peroxide. The reduction of the peroxide to form OH^- can be achieved by peroxide decomposers (*e.g.*, metal oxides). The second generation IHS air cathodes contain no noble metals [24]. Figures 10 and 11 compare the performance of the electrodes at 50, 75, 100 and 150 mA cm^{-2} with air as a function of the operating temperature. It is obvious that both types of electrodes show comparable performance, even at room temperature. Electron microscopy and mercury intrusion porosimetry were used to optimize structural parameters of the electrodes. Figure 12 shows a scanning electron microscope graph of a microtome cut of an air cathode. Figure 13 shows the pore size distribution curve for the cathode diffusion layer. The peak at about 0.1 μm corresponds to the internal pore structure of the Shawinigan SH 100 carbon. The pore system created by the filler (100 μm) lies beyond the resolution of the instrument used. Figure 14 shows the pore size distribution for the cathode catalyst layer. The peak at 0.03 μm was found to be characteristic of the internal

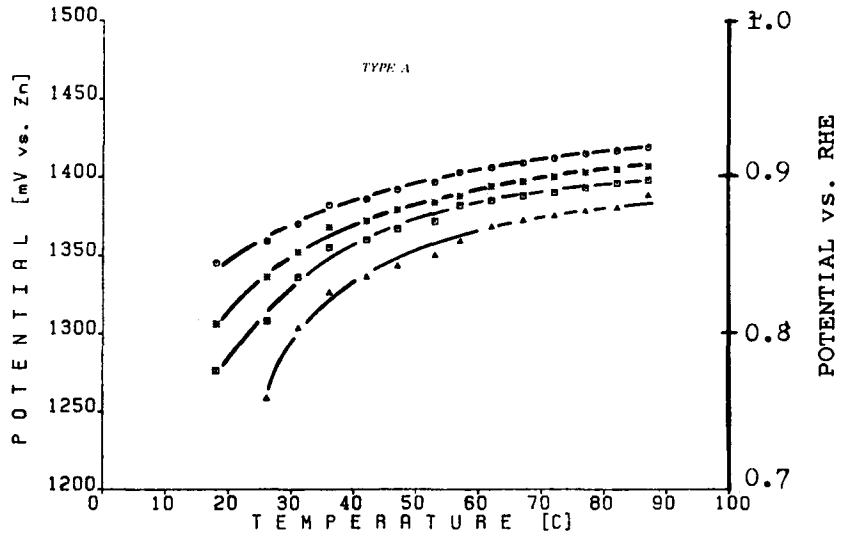

Fig. 10. Operating voltage for the 1st generation air cathode as a function of temperature for air operation at different current densities. ○, 50 mA cm^{-2}; *, 75 mA cm^{-2}; □, 100 mA cm^{-2}; ▲, 150 mA cm^{-2}.

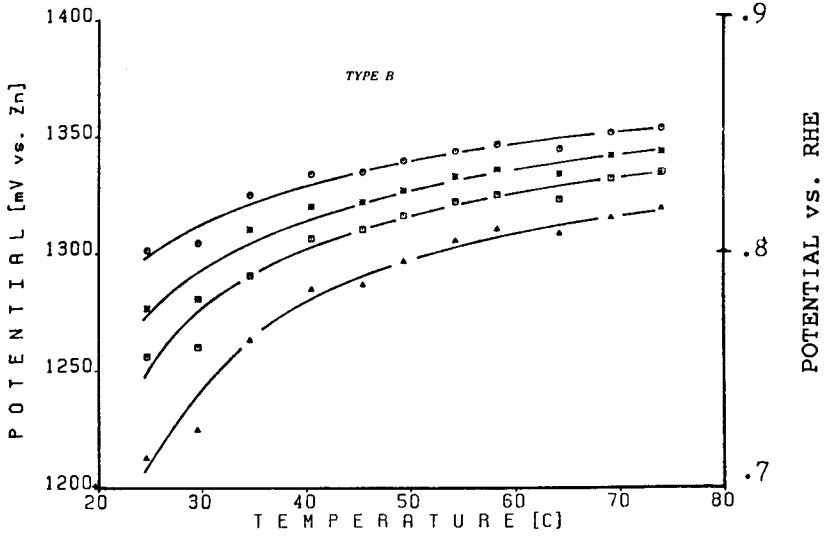

Fig. 11. Operating voltage for the 2nd generation air cathode as a function of temperature for air operation at different current densities. ○, 50 mA cm^{-2}; ✱, 75 mA cm^{-2}; □, 100 mA cm^{-2}; ▲, 150 mA cm^{-2}.

Fig. 12. SEM graph of an air-cathode cross-section, 1, Backing; 2, gas diffusion layer; 3, catalyst layer.

pore system of Vulcan XC 72R. Figure 15 shows the mercury intrusion curve for the air cathode (including the carbon cloth backing). Apart from the characteristic carbon peaks (microstructure) the pore structure created by the Teflon bonded carbon particles (macrostructure) becomes obvious.

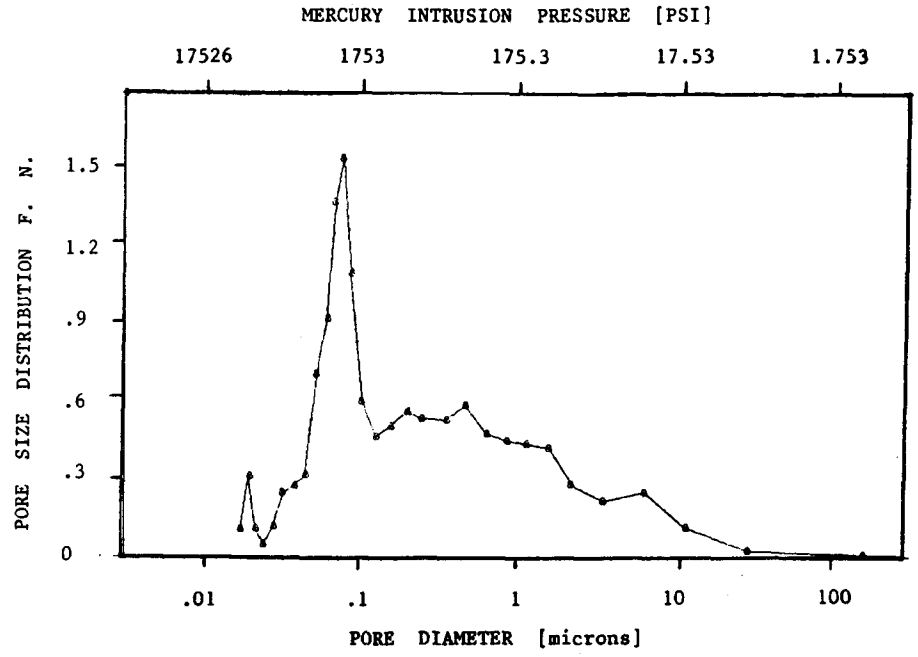

Fig. 13. Pore size distribution of an air cathode diffusion layer.

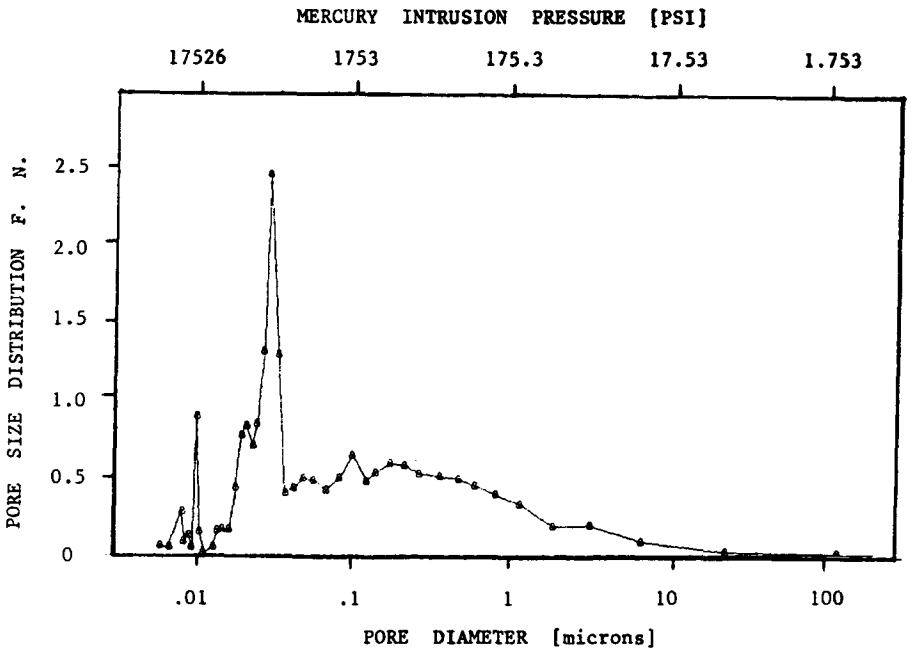

Fig. 14. Pore size distribution of an air cathode catalyst layer.

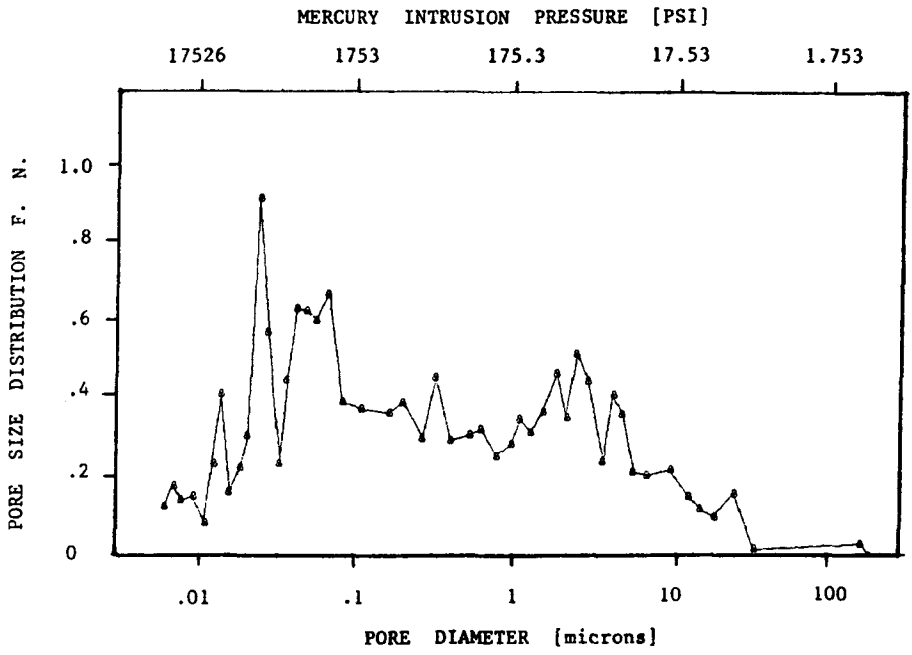

Fig. 15. Pore size distribution of an air cathode.

Hydrogen electrodes are post-catalyzed with a mixture of palladium and rhodium. As the activity of the noble metal catalyst depends on its surface area rather than its weight, care is taken that the noble metal salt reduction leads to small catalyst particles (below 10 nm). The first generation anodes contained 1.0 mg Pd/Rh per cm^2. In the second generation the catalyst loading has been reduced to 0.5 mg Pd/Rh per cm^2 while maintaining the electrode performance. Presently, it is not clear whether the anode electrocatalyst loading can be reduced by the use of precatalyzed carbon-supported Pd/Rh rather than by applying the post-catalyzation method. Figure 16 shows a scanning electron microscope graph of a microtome cut of an anode. As Black Pearls 2000 is used for both the diffusion and the catalyst layer of the anode, mercury intrusion curves for the individual layers do not vary significantly from the one obtained for the finished electrode (Fig. 17). The pore size distribution curve of the anode catalyst layer obtained with 12 N KOH as intrusion fluid shows that all but very small pores have been filled with electrolyte in the process of filling the sample test cell with the intrusion liquid (5 psi) (Fig. 18). Electron microscopic investigations of the penetration depth of the electrolyte into the electrode confirmed that KOH penetrates the anode through the entire catalyst layer and stops at the diffusion layer.

Figures 19 and 20 show the cost analysis for the first two generation electrodes. Second generation electrodes represent a great reduction in

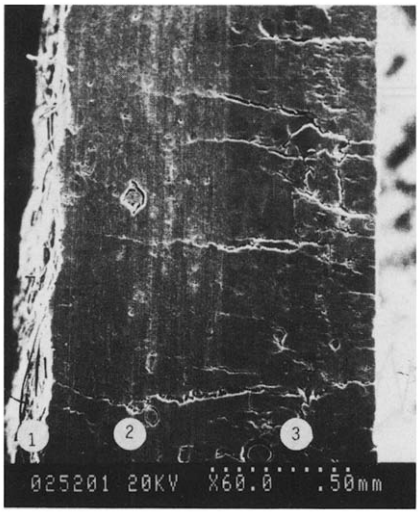

Fig. 16. SEM graph of a hydrogen anode cross-section. 1, Backing; 2, diffusion layer; 3, catalyst layer.

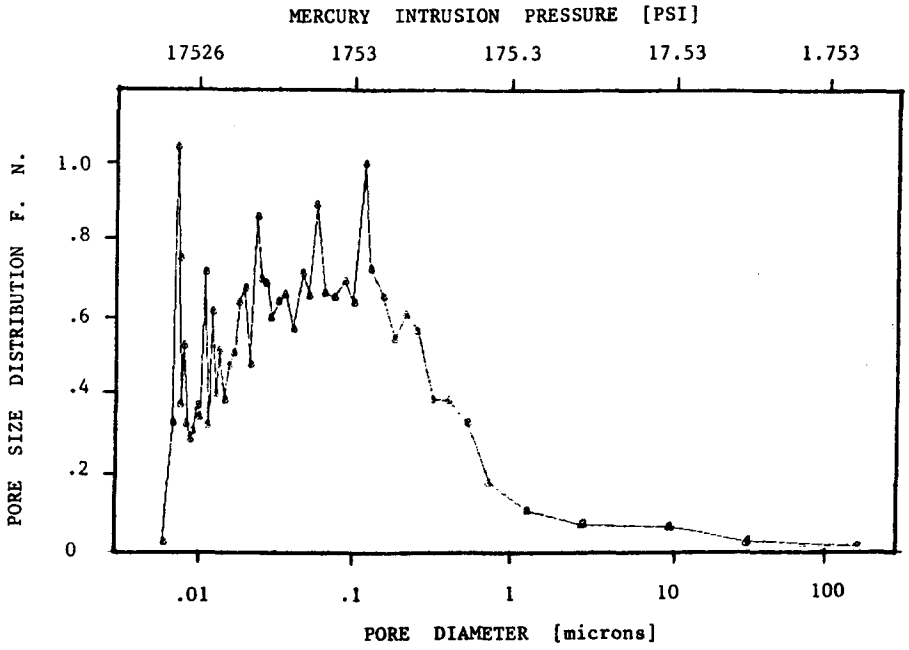

Fig. 17. Pore size distribution of an anode catalyst layer using mercury intrusion.

material cost. Both, first generation electrodes ("cost 1") using 0.5 mg of Pt per cm^2 on the cathode and 1 mg per cm^2 of Pd/Rh on the anode, and second generation ("cost 2") electrodes using no noble metal electrocatalyst

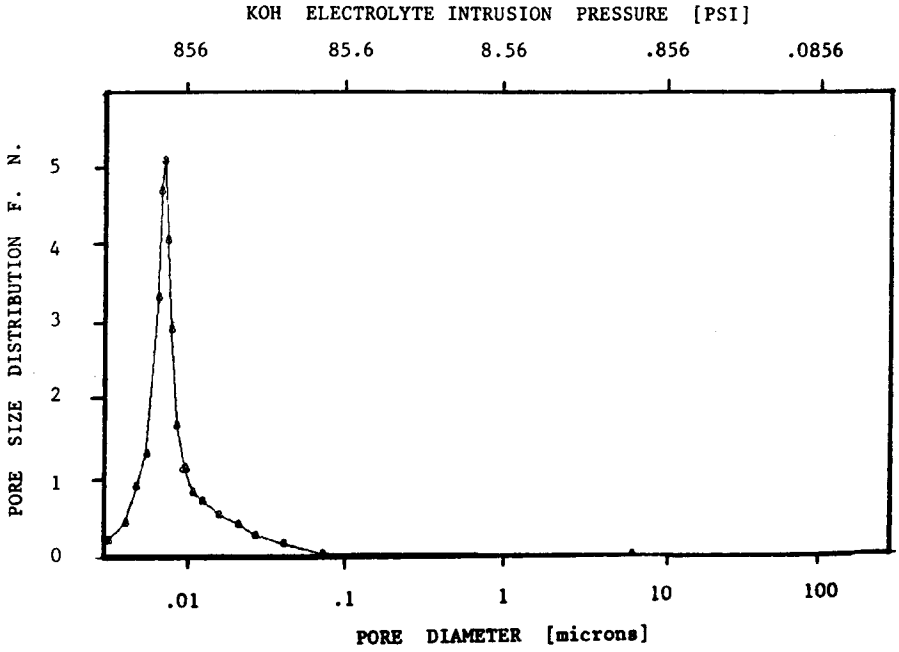

Fig. 18. Pore size distribution of an anode catalyst layer using 12 N KOH as intrusion liquid.

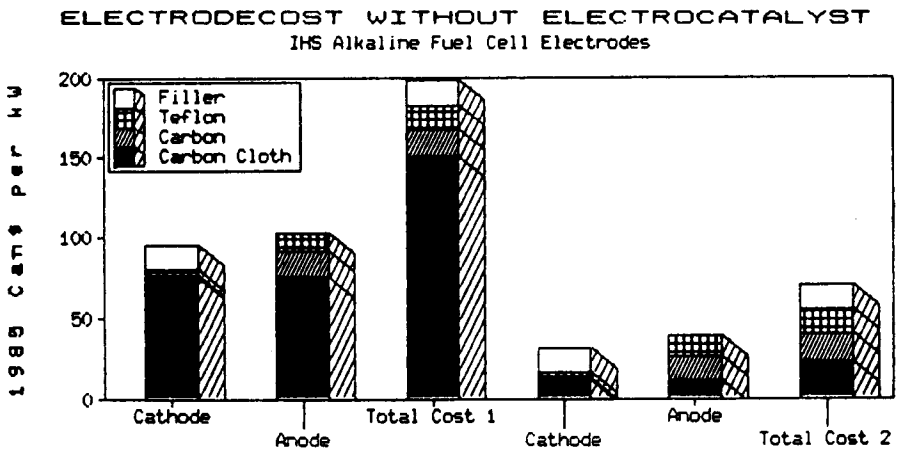

Fig. 19. Cost analysis based on power for the IHS gas diffusion electrodes.

on the cathode and 0.5 mg of Pd/Rh per cm^2 on the anode, satisfied the set 2000 h lifetime goal. The cost figures are based on the purchase of 10 kg or less of the raw material (250 g for 10% Pt on carbon).

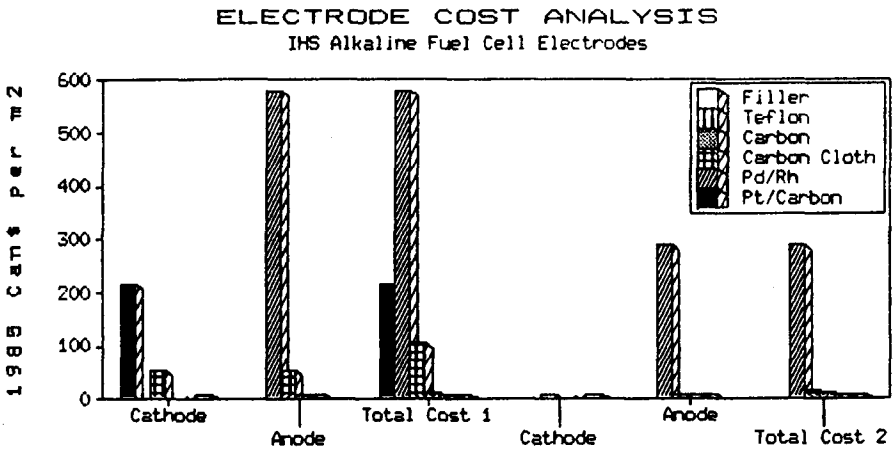

Fig. 20. Cost analysis based on electrode area for the IHS gas diffusion electrodes.

Electrode fabrication and evaluation

The electrode manufacturing process currently used is shown in Fig. 21. First, the electrode backing is chosen. In the case of carbon cloth or carbon paper, the material is wetproofed with Teflon suspension to a loading of 50% Teflon by weight. The diffusion layer is prepared by mixing the appropriate amounts of carbon, Teflon, and a suspension agent (*e.g.*, light fraction of petrol). A filler (sugar or ammonium bicarbonate) is added to adjust porosity. This mixture is homogenized and, after filtering off the suspension agent, a workable dough is obtained. The procedure is repeated with a modified composition for the catalyst layer. Thin foils are prepared using a cross-rolling technique. The thickness of the foils is adjusted using spacers. Individual layers are cut to size, then the three layers are assembled and cross-rolled together. After pressing, the filler is removed by washing (sugar) or drying at 100 °C (bicarbonate). The electrode is sintered under slight pressure at 320 °C for 20 min [25].

Performance testing analyzes the polarization behavior of anodes and cathodes, as well as lifetimes. A new measuring circuit for the determination of resistance-free voltages under load was used [26, 27]. Figure 22 shows the *IR*-free, single-cell performance for the hydrogen–oxygen and the hydrogen–air cell at 65 °C (12 N KOH). Tests indicate that at a current density of 100 mA cm^{-2}, the *IR*-free cell voltages are 0.9 V with oxygen and 0.85 V with air as cathode reactant. At the nominal current density (100 mA cm^{-2}), the difference between oxygen and air operation is around 50 mV. The resistance free voltage difference between oxygen and air performance is used as a measure of the deterioration during aging. So far close to 4000 h of continuous operation have been achieved with air cathodes (Fig. 23) and

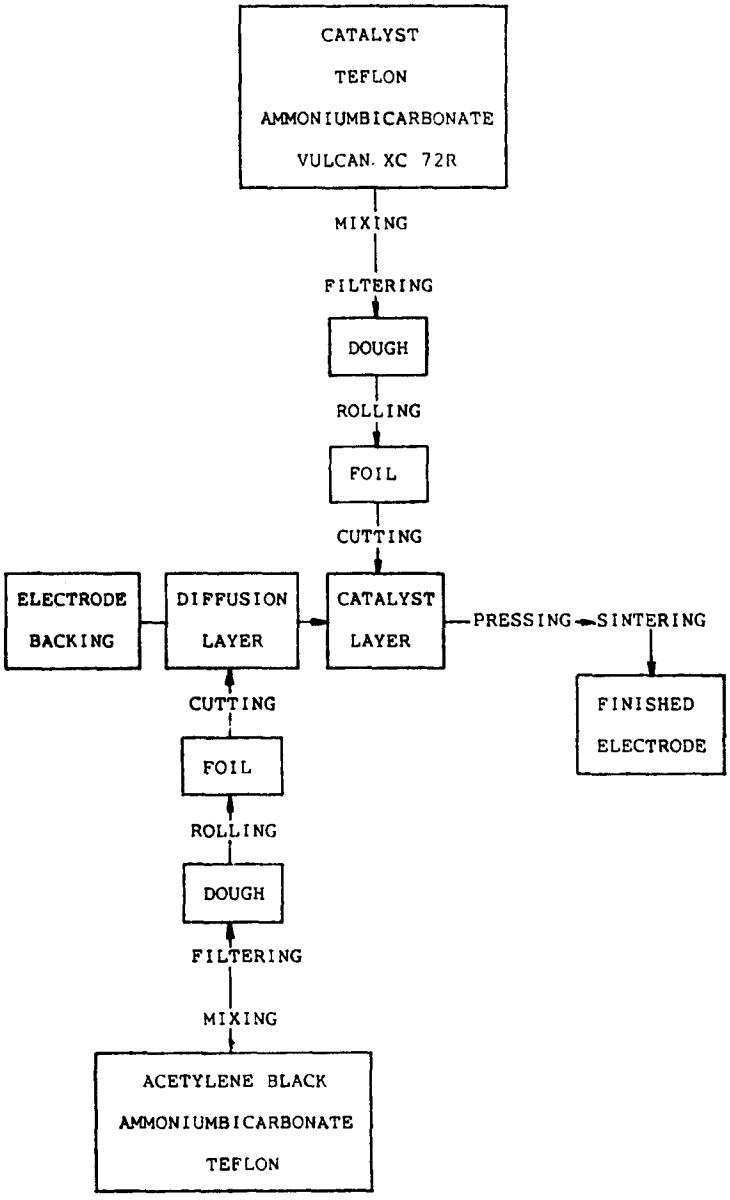

Fig. 21. Flow sheet for the production of IHS Teflon bonded multilayer electrodes.

hydrogen anodes (Fig. 24). Electrode lifetimes under intermittent operation have not been investigated yet as, after use, the fuel cell will be purged with nitrogen and/or the electrolyte drained, thus avoiding carbon corrosion in the air cathode at oxygen rest potential. In the next stage of the program,

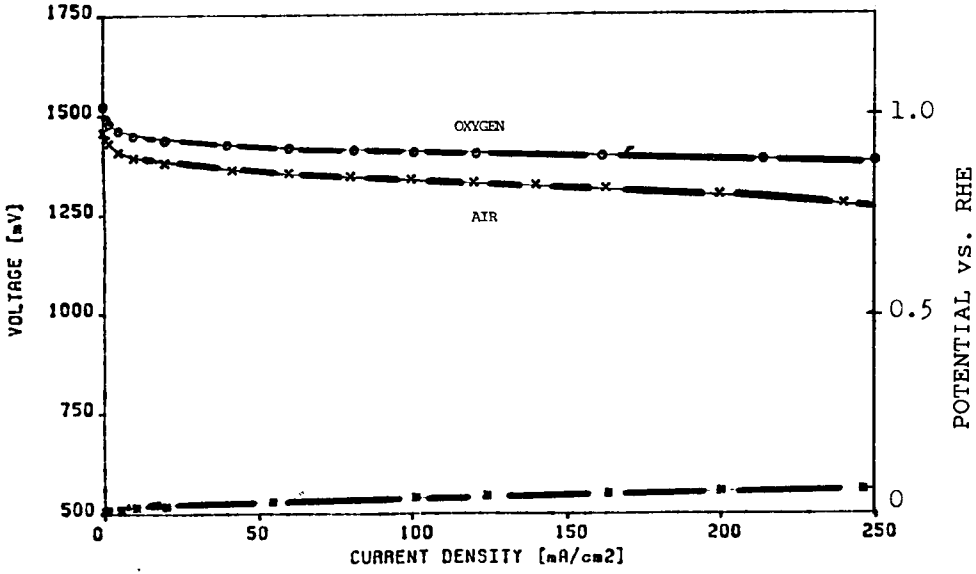

Fig. 22. *IR* free single cell performance of the hydrogen–oxygen and the hydrogen–air alkaline fuel cell (12 N KOH, 65 °C).

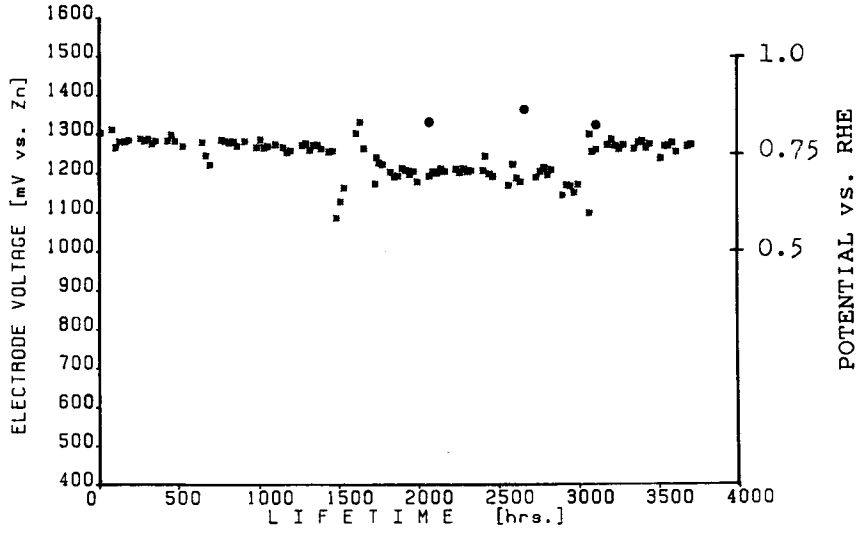

Fig. 23. Lifetime of a batch 502 IHS cathode with air as reactant (65 °C, 12 N KOH, 100 mA cm^{-2}).

however, electrode performance under "operating conditions" will be determined using a simulated load pattern including open circuit standby and short periods of overload.

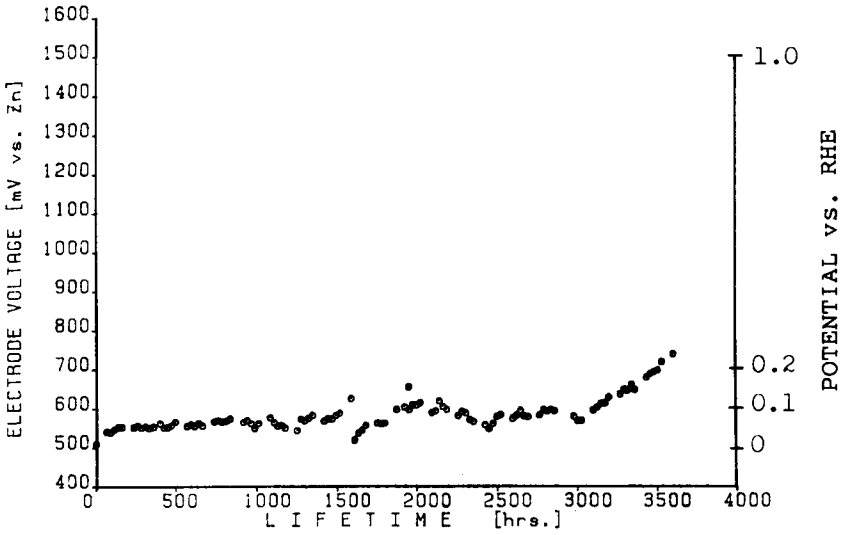

Fig. 24. Lifetime of a batch 17H2 IHS anode (65 °C, 12 N KOH, 100 mA cm^{-2}).

Conclusion

The IHS alkaline bipolar hydrogen–air fuel cells have reached a high status of development. Carbon material selection and pretreatment for Teflon bonded multilayer electrodes was found to be of prime importance. Electrode fabrication methods have been developed on the laboratory scale. Electrode life of over 3500 h at 100 mA cm^{-2} have been achieved with air cathodes and hydrogen anodes. Conductive plastics have been introduced as low cost construction materials which can be formed by mass production methods (extrusion and/or injection moulding).

Acknowledgement

This work was supported by the Ontario Ministry of Energy (OMENG). The authors thank Dr S. Srinivasan of the Los Alamos National Laboratory, Los Alamos, New Mexico, for his interest and encouragement of this work. They also thank Astris Science Inc. for granting permission to publish this paper.

References

1 D. S. Scott, D. McCammond, C. A. Ward, G. C. Weatherly, R. D. Venter and J. S. Wallace, Study of fuel cells analysis options for their development in Canada — Phase II, prepared for the Defense Research Establishment, Ottawa, and Transport Canada, Ottawa, July, 1980.

2 H. Maru, L. Christner, S. Abens and B. Baker, Phosphoric acid fuel cell technology, *National Fuel Cell Seminar, 1979.*
3 A. J. Appleby, Acid fuel cell technology — an overview, *National Fuel Cell Seminar, 1983, Abstracts*, pp. 1 - 6.
4 L. Handley, Status of 40 kW and 4.8 MW fuel cell program, National Fuel Cell Program, *National Fuel Cell Seminar, 1979.*
5 L. Gelfond, 4.8 MW demonstrator: a progress report, *National Fuel Cell Seminar, 1983, Abstracts*, pp. 51 - 55.
6 J. F. McElroy, Solid polymer electrolyte fuel cell technology, *National Fuel Cell Seminar, 1978.*
7 J. F. McElroy, Status of solid polymer electrolyte fuel cell technology, *National Fuel Cell Seminar, 1983, Abstracts*, pp. 123 - 127.
8 D. W. Sheibley, J. D. Denais and L. S. Murgia, NASA fuel cell applications for space, *National Fuel Cell Seminar, 1983, Abstracts*, pp. 107 - 110.
9 A. T. Emery, Oxy-hydrogen–air fuel cell, *National Fuel Cell Seminar, 1983, Abstracts*, pp. 98 - 103.
10 H. Van den Broeck, L. Adriaensen, M. Alfenaar, A. Beekman, A. Blanchart, G. Van Bogaert and G. Vanneste, Status of Elenco's alkaline fuel cell development, Hydrogen Energy Progress V, *Proc. 5th World Hydrogen Conf., Toronto, Canada, July 15 - 20, 1985*, Vol. 4. pp. 1669 - 1676.
11 R. D. Pierce, J. P. Ackerman, Molten carbonate fuel cells — development status, *National Fuel Cell Seminar, 1983, Abstracts*, pp. 6 - 11.
12 D. C. Fee and J. P. Ackerman, Solid oxide fuel cells, *National Fuel Cell Seminar, 1983, Abstracts*, pp. 11 - 15.
13 R. Findlay, L. Jones and P. Hyde, Canadian opportunities for alkaline fuel cells, *IHS Report, June, 1985.*
14 K. V. Kordesch, 25 Years of fuel cell development (1951 - 1976), *J. Electrochem. Soc., 125* (1978) 271 - 283.
15 K. V. Kordesch and Ch. Fabian, Battery/fuel cell hybrid electric vehicle, in D. A. J. Rand (ed.), *Power Sources for Electric Vehicles*, Elsevier, Amsterdam, 1983.
16 K. Tomantschger, R. Findlay, P. Hyde, I. Ioanes, F. McClusky, L. Oporto, A. Reid and K. Kordesch, Analysis of the internal resistance of the Institute for Hydrogen System's bipolar alkaline fuel cell, *The Electrochemical Society Spring Meeting, Boston, MA, May 4 - 9, 1986, Extended Abstracts*, in press.
17 K. Kordesch, J. Gsellmann, R. Findlay, S. Srinivasan and K. Tomantschger, Electrode designs and concepts for bipolar, alkaline fuel cells, Hydrogen Energy V, *Proc. 5th World Hydrogen Conf., Toronto, Ontario, July 15 - 20, 1984*, Vol. 4, pp. 1657 - 1668.
18 K. Tomantschger, K. Kordesch, L. Oporto and S. Srinivasan, Status of the 500 watt alkaline fuel cell development project, Part I: electrode fabrication and evaluation, *The Electrochemical Society Spring Meeting, Toronto, Ontario, May 12 - 17, 1985, Extended Abstracts No. 306*, pp. 441 - 442.
19 K. V. Kordesch, J. Gsellmann, S. Jahangir and M. Schautz, The technology of PTFE-bonded carbon electrodes, *The Electrochemical Society Fall Meeting, Detroit, MI, October 17 - 21, 1982, Extended Abstracts No. 265*, pp. 427 - 428.
20 K. Kordesch, Survey of carbon and its role in phosphoric acid fuel cells, *Final Rep., Brookhaven National Laboratory, December, 1979.*
21 K. Tomantschger, K. Kordesch, P. Hyde, L. Oporto, A. Reid and S. Srinivasan, Selection and pretreatment of carbon materials for gas diffusion electrodes, *The Electrochemical Society Spring Meeting, Toronto, Ontario, May 12 - 17, 1985, Extended Abstracts No. 646*, p. 904.
22 K. Tomantschger, K. Kordesch, P. Hyde, L. Oporto, A. Reid and S. Srinivasan, Selection and pretreatment of carbon materials for gas diffusion electrodes, *IHS Rep., 1986.*
23 K. Tomantschger, K. Kordesch, F. McClusky, L. Oporto, A. Reid and S. Srinivasan,

Stability of carbon in alkaline electrolytes, *The Electrochemical Society Fall Meeting, Las Vegas, NV, October 13 - 18, 1985, Extended Abstract No. 41*, pp. 65 - 66.

24 K. Kordesch and K. Tomantschger, Metal oxide catalysed electrodes, patent disclosure, to be filed.

25 K. Tomantschger and L. Oporto, Fabrication procedures for the IHS gas diffusion electrodes, *IHS Report*, June, 1985.

26 K. V. Kordesch and A. Marko, Sine wave pulse current tester for batteries, *J. Electrochem. Soc., 107* (1960) 480 - 483.

27 K. V. Kordesch and J. Gsellmann, An improved interrupter circuit for battery testing, a function generator for the resistance free reading of current–voltage curves, *J. Electrochem. Soc., 132* (1985) 747 - 751.